OXFORD UNIVERSITY PRESS | Journal of Plankton Research

RNA/DNA ratios as estimate of metabolic and functional traits in diatom species from the Northwestern Adriatic Sea

Journal:	*Journal of Plankton Research*
Manuscript ID	Draft
Manuscript Type:	Original Article
Date Submitted by the Author:	n/a
Complete List of Authors:	Casabianca, Silvia; University of Urbino Department of Biomolecular Sciences, Department of Biomolecular Sciences Capellacci, Samuela; University of Urbino, Department of Biomolecular Sciences Ricci, Fabio; University of Urbino Department of Biomolecular Sciences, Department of Biomolecular Sciences Ravera, Giorgia; University of Urbino, Department of Pure and Applied Sciences Signa, Geraldina; Università degli Studi di Palermo, Department of Earth and Marine Sciences Scardi, Michele; University of Tor Vergata, Department of Biology Penna, Antonella; University of Urbino, Dipartimento di Scienze Biomolecolari
Keywords:	Adriatic Sea, 18S rRNA/rDNA ratio, RNA/DNA ratio, Diatoms, Biomass, Metabolic dynamics

Dr. Silvia Casabianca
Department of Biomolecular Sciences, University of Urbino, Campus E. Mattei, 61029 Urbino (PU), Italy
Tel. +39 0722 304907
e-mail: silvia.casabianca@uniurb.it
http://www.marine-ecology.uniurb.it

Dear Editor in Chief of Journal of Plankton Research,

here attached, please find electronic version of the manuscript entitled "RNA/DNA ratios as estimate of metabolic and functional traits in diatom species from the Northwestern Adriatic Sea" by Silvia Casabianca, Samuela Capellacci, Fabio Ricci, Giorgia Ravera, Geraldina Signa, Michele Scardi, Antonella Penna.

This work has not been submitted to any other journal and there are no outstanding related publications pending. All authors are aware of, and accept responsibility for, the manuscript.

The study regards the relationship between metabolic activity variation based on RNA/DNA ratio and taxon-specific 18S rRNA/DNA ratio of target marine diatoms from the Adriatic Sea. We tested the hypothesis if these molecular variables can describe the metabolic dynamics of phytoplankton species during their growth phase. The aim of this study was to investigate if the RNA/DNA and taxon-specific 18S rRNA/rDNA ratios could be used to assess and be indicators of metabolic activity in marine phytoplankton species, such as two Adriatic diatom species, *Chaetoceros socialis* and *Skeletonema marinoi* and to verify if these ratios could reflect, and thus can be used to predict, biomass growth and metabolic dynamics in marine phytoplankton species.

Rationale: Different phytoplankton biomass estimations can provide information on abundance variation, while they are not able to describe the metabolic activity of species or groups within assemblages. Conversely, molecular traits are key for the metabolic dynamics in pelagic ecosystems. To investigate if the RNA/DNA and taxon-specific 18S rRNA/rDNA ratios could be used to assess and be indicators of metabolic activity in marine phytoplankton species, two Adriatic diatom species, *Chaetoceros socialis* and *Skeletonema marinoi* were studied. Significant correlations between abundance, chlorophyll *a*, carbon content and proteins were found in individual and co-cultured growth experiments (from r_s=0.570 to r_s =0.986, P<0.001). Biomass trend followed the logistic curve without prove additional information regarding diatom metabolic activity. In both experiments, the RNA/DNA and taxon-specific 18S rRNA/rDNA ratios of *C. socialis* and *S. marinoi* showed maximum values at the beginning of the growth phase, i.e, as 23.2±1.5 and 15.3±0.8, and 16.2±1.6 and 30.1±5.4 after 2 and 6 days, respectively, in individual culture, with a subsequent significant decrease values for both species in individual and co-culture experiments. Our results showed that these molecular rRNA/rDNA ratios expressed an activation of metabolism, before the abundance increases, also within the interspecific interaction between *C. socialis* and *S. marinoi*.

Author contributions
All authors made a substantial contribution to the study in terms of conception, data acquisition, or analysis; contributed substantially to drafting the manuscript; and approved the final submitted manuscript.

We would be glad if you can consider the manuscript for publication in *Journal of Plankton Research.*

We think that *Journal of Plankton Research* is the best outlet for our work since this paper deals with metabolic dynamics of phytoplankton species during their growth phase analysed by experimental setup of phytoplankton species from North-western Adriatic Sea using RNA/DNA and taxon-specific 18S rRNA/DNA ratios approach.

Urbino, 27 June 2023,

Sincerely Yours,
Dr. Silvia Casabianca, Ph.D

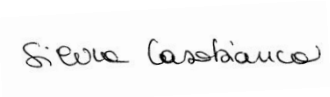

RNA/DNA ratios as estimate of metabolic and functional traits in diatom species from the Northwestern Adriatic Sea

Running Head: Phytoplankton RNA/DNA ratio for metabolic dynamic

Silvia Casabianca[1,2,3*], Samuela Capellacci[1,2,3], Fabio Ricci[1,2,3], Giorgia Ravera[4], Geraldina Signa[2,5], Michele Scardi[2,6], Antonella Penna[1,2,3]

[1]Department of Biomolecular Sciences, University of Urbino, 61029 Urbino, Italy
[2]CoNISMa, National Inter-University Consortium for Marine Sciences, 00196 Rome, Italy
[3]Fano Marine Center, The Inter-Institute Center for Research on Marine Biodiversity, Resources and Biotechnologies (FMC), 61032 Fano, Italy
[4]Department of Pure and Applied Sciences, University of Urbino, 61029 Urbino, Italy
[5]Department of Earth and Marine Sciences, University of Palermo, Palermo, Italy
[6]Department of Biology, University of Tor Vergata, 00133 Rome, Italy

*Corresponding author: silvia.casabianca@uniurb.it

Abstract

Different phytoplankton biomass estimations can provide information on abundance variation, while they are not able to describe the metabolic activity of species or groups within assemblages. Conversely, molecular traits are key for the metabolic dynamics in pelagic ecosystems. To investigate if the RNA/DNA and taxon-specific 18S rRNA/rDNA ratios could be used to assess and be indicators of metabolic activity in marine phytoplankton species, two Adriatic diatom species, *Chaetoceros socialis* and *Skeletonema marinoi* were studied. Significant correlations between abundance, chlorophyll a, carbon content and proteins were found in individual and co-cultured growth experiments (from r_s=0.570 to r_s =0.986, P<0.001). Biomass trend followed the logistic curve without prove additional information regarding diatom metabolic activity. In both experiments, the RNA/DNA and taxon-specific 18S rRNA/rDNA ratios of *C. socialis* and *S. marinoi* showed maximum values at the beginning of the growth phase, i.e, as 23.2±1.5 and 15.3±0.8, and 16.2±1.6 and 30.1±5.4 after 2 and 6 days, respectively, in individual culture, with a subsequent significant decrease values for both species in individual and co-culture experiments. Our results showed that these molecular rRNA/rDNA ratios expressed an activation of metabolism,

before the abundance increases, also within the interspecific interaction between *C. socialis* and *S. marinoi*.

KEY WORDS: Adriatic Sea, 18S rRNA/rDNA ratio; RNA/DNA ratio; Biatoms; Biomass; Metabolic dynamics

INTRODUCTION

In the pelagic and coastal ecosystems, phytoplankton are the main primary producers that gather sunlight through photosynthesis to produce chemical energy, which is thus, transferred throughout the trophic web (Falkowski, 2002; Brett et al., 2009; Marra, 2009). Marine photosynthetic plankton are responsible for the production of approximately 50 petagrams (10^{15}) of carbon per year, an amount comparable to that found on land (Chavez et al., 2011).

In marine environment, phytoplankton morphological, biochemical and molecular traits, such as cell size and shape, macromolecules composition in proteins, polysaccharides, lipids, nucleic acids, can play an important role in determining, in terms of energy content, phytoplankton ecological niches and phytoplankton species coexistence. These processes can be influenced by light and nutrient assimilation, leading to biomass increase, and influencing sinking and grazing processes (Chícharo and Chícharo, 2008; Litchman and Klausmeier, 2008; Follows and Dutkiewicz, 2011; Naselli-Flores and Barone, 2011; Finkel et al., 2016; Garcia et al., 2016). In fact, different functional traits can represent adaptive strategy to various environmental conditions (Kruk et al., 2010; Roselli and Basset, 2015). Further, environmental conditions can affect the ecophysiology of phytoplankton assemblages. Growth rate and protein, DNA and RNA content variability are linked to nitrogen decreasing and, instead, carbohydrates and lipids increase under nitrogen starvation (Flynn et al., 2010; Loladze and Elser, 2011). The increase in growth rate is related to the increase of RNA content and relative protein concentration, as well as the ribosomal RNA (rRNA) content is linked to requirements for protein synthesis and synthesis rate of ribosomes (Flynn et al., 2010; Loladze and Elser, 2011; Daines et al., 2014). Thus, the rRNA content is indicative of the growth, metabolism, or overall activity of a cell and may be used for the estimation of these parameters (Blazewicz et al., 2013). According to the growth rate hypothesis, which takes into account the relationship between cell size and biomass growth, smaller phytoplankton cells require more RNA and protein content than larger phytoplankton cells (Marañón et al., 2012; Daines et al., 2014).

In field, nucleic acids, proteins, carbohydrates, lipids and secondary metabolites that are biochemical components of photosynthetic production can be used to assess actively growing

natural assemblages (Nejstgaard et al., 2003; Berdalet et al., 2005; Ikeda et al., 2007; Finkel et al., 2016). It has previously been shown that the diatom and dinoflagellate 18S rRNA/rDNA ratios measured within phytoplankton assemblages were significantly correlated to biomass, and because this molecular parameter is linked to cellular RNA variability, it has the potential to express the growth rate and metabolic dynamics of phytoplankton assemblages (Dortch et al., 1983; Nicklisch and Steinberg, 2009; Casabianca et al., 2021).

In the present study, the metabolism in terms of molecular rRNA/rDNA ratio dynamics and biomass trend during the various phases of phytoplankton growth have been thoroughly studied to understand if the 18S rRNA/rDNA ratio could be used to assess species-specific metabolic activity and, consequently, phytoplankton assemblage functioning in marine coastal ecosystem.

Phytoplankton species under investigation have been selected based on the composition of phytoplankton assemblages in Northwestern Adriatic Sea. Seasonal diatom blooms, which are frequently monospecific or mixed by co-occurring dominating diatom taxa, such as *Chaetoceros* spp. and *Skeletonema marinoi*, are of importance in this Adriatic region (Cabrini et al., 2012; Totti et al., 2019; Casabianca et al., 2021; Casabianca et al., 2022; Neri et al., 2023). The high-density blooms are sustained by nutrient availability from turbulent waters and riverine inputs from both Po and minor river discharges (Bernardi Aubry et al., 2004; Penna et al., 2004; Mangoni et al., 2008; Socal et al., 2008; Mangoni et al., 2013; Penna et al., 2013; Ricci et al., 2022), as well as diatom high nutrient uptake rates (Litchman et al., 2007).

In the present study, the hypothesis of the application of RNA/DNA ratio and taxon-specific 18S rRNA/rDNA ratio on target diatom species for the metabolic activity evaluation in culture systems was tested. The total RNA/DNA ratios based on nucleic acid quantification and 18S rRNA/rDNA ratio based on molecular qPCR-based assay, respectively, were estimated along the growth phases in both diatom individual and co-culture systems. Finally, the aim of this study was to verify if these ratios can be indicator of metabolic status in marine phytoplankton species at the early phase of the active reproduction.

MATERIALS AND METHODS

Microalgal cultures and abundance determination

Diatom *Chaetoceros socialis* CBA22 and *Skeletonema marinoi* CBA4 strains, isolated from Adriatic Sea, were maintained in sterilized f/2 medium (Guillard, 1975) and incubated at 18 ± 1 °C with a light:dark cycle of 12:12 h and a light intensity of 100 µmol $m^{-2}s^{-1}$. Cultured experiments were performed in 1 L glass flasks containing 400 mL of the ASPM (Artificial Seawater Provasoli-McLachlan) base (Guillard, 1975) enriched with f/2 medium. Cells were kept in suspension by manually mixing each flask almost twice a day. Medium nutrient concentrations were maintained

constant (see below). *C. socialis* CBA22 and *S. marinoi* CBA4 were grown either individually or together in co-culture systems for 24 and 30 days, respectively. Culture subsamples were fixed with Lugol's iodine solution and cell abundance (cell mL^{-1}) was determined every two days using the Sedgewick-Rafter methods (LeGresley and McDermott, 2010) under an inverted microscope (Zeiss Axiovert 40 CFL, Germany) equipped with phase contrast. Further, diatom biomass expressed as total carbon content per each species (mg C L^{-1}), was also estimated through cellular volume as reported in Menden-Deuer and Lessard (2000).

Diatoms growth rates μ, defined as the instantaneous rate of increase, were calculated on the basis of the longest possible period of exponential growth using the equation: $\mu = \ln (Nt/N0)/\Delta t$, where N is the number of cells mL^{-1}, Δt is the time interval (Wood et al., 2005). Cultured subsamples of both diatom species, each containing 1.0×10^6 total cells were harvested every two days by centrifugation (4000 rpm for 10 min) during the growth phase. The obtained microalgal pellets were stored at -80 °C until nucleic acid and protein extraction analyses. All the experiments were carried out in triplicate.

Analysis of chlorophyll *a* of diatom cultured strain

Biomass determination was also assessed by chlorophyll *a* (chl *a*) content. Amounts of 10 mL of each diatom strain of *C. socialis* CBA22 and *S. marinoi* CBA4 and co-cultured diatom strains were centrifuged (4000 rpm for 10 min) and spectrofluorimetric analyses of chl *a* were performed following Yentsch and Menzel (1963) and Holm-Hansen et al. (1965) methods using a Shimatzu spectrofluorometer (Skimatzu RF-6000, Japan). The pigment quantification was carried out using a standard chl *a* from spinach solution (Life Science, Merck, Germany).

Nutrient analyses

In order to maintain the constant nutrient values, chemical analyses of dissolved inorganic nutrients ($N\text{-}NO_3$, $N\text{-}NO_2$, $N\text{-}NH_4$, $P\text{-}PO_4$ and $Si\text{-}SiO_2$) were performed every two days during the growth phase. Nutrients concentration was evaluated in culture medium sub-samples after a filtration step on 0.45 μm nitrocellulose filters (Millipore, Temecula, CA, USA) following the method of Strickland and Parsons (1972) and using a Shimadzu spectrophotometer (mod. UV-1700, Japan). Following the nutrient concentration of f/2 medium (Guillard, 1975), $NaNO_3$, NaH_2PO_4 and Na_2SiO_3 were kept in the media of cultured and co-cultured diatoms roughly at 8.82×10^{-4} M, 3.62×10^{-5} M and 1.06×10^{-4} M, respectively.

Nucleic acids and protein extraction, qPCR assay, taxon and genus-specific 18S rRNA/rDNA ratio calculation and target amplicon sequencing

Total genomic DNA, RNA and proteins from individual and co-cultured cultured samples of *C. socialis* CBA22 and *S. marinoi* CBA4 were extracted using the RNA/DNA/Protein Purification Plus Kit (Norgen Biotek Corp., Thorold, Canada) according to the manufacturer's instructions. The nucleic acids and proteins quantification and the cDNA preparation protocols were reported in Casabianca et al. (2021). The diatoms 18S rRNA/rDNA ratio was calculated using class-specific primers targeting diatoms taxa (Casabianca et al. 2021), while *Chaetoceros* spp. and *Skeletonema* spp. 18S rRNA/rDNA ratio were obtained using new primers targeting 18S rDNA gene of both genera (this study). These new primers were designed on sequences available from GenBank using Primer-BLAST (Ye et al., 2012). Multiple sequence alignments were carried out using CLUSTALX2 v. 2.0 (Larkin et al., 2007). The specificity of the new primers was tested *in silico* using BLAST (Basic Local Alignment Search Tool). The qPCR reactions were performed in a final volume of 25 µL using the Hot-Rescue Real Time PCR Kit-SG (Diatheva, Fano, Italy) with 1 µL undiluted and 1:10 diluted DNA and cDNA templates. Taxon-specific primer sequences, primers and $MgCl_2$ concentrations, amplicon melting temperatures and sizes are shown in Table S1. The thermal cycling conditions consisted of 10 min at 95 °C, followed by 40 cycles at 95 °C for 15 s and 60 °C for 1 min. All amplification reactions were carried out in a StepOne Real-Time PCR System (Applied Biosystems, Foster City, CA, USA). All samples were run with three biological replicates, each of which was run with two technical replicates. In all experiments, negative controls containing MilliQ water were tested. At the end of each run, a melting curve analysis was performed to exclude the presence of primer dimers or non-specific amplified products. Standard curves for the two new primer sets were constructed using a 6-point tenfold dilution series of purified rDNA PCR products (from 2 to 1.0×10^6 copies) generated from DNA and cDNA of the target species as described in Perini et al. (2019). Acquisition of the qPCR data and subsequent analyses were carried out using StepOne Software ver. 2.3. Standard curves were created automatically and accepted when the slopes were between −3.58 and −3.32 (90–100% efficiency) and the determination coefficient (r^2) was at least 0.99. Amplification efficiency was calculated as $(10^{(-1/\text{slope})} - 1) \times 100$. The 18S rRNA/rDNA ratio calculation for each target species was performed as reported in Casabianca et al. (2021).

The qPCR amplified products were sequenced to confirm the expected sequences. The 18S rDNA fragments were amplified and sequenced using Chaet_spp_F, Chaet_spp_R and Skel_spp_F, Skel_spp_R (Table S1). All amplified PCR products were purified using the MinElute Gel Extraction Kit (Qiagen), and the products were directly sequenced with the ABI PRISM BigDye Terminator Cycle Sequencing Kit v.1.1 on an ABI 310 Genetic Analyzer (Applied Biosystem, Foster City, CA, USA). Standard thermal cycling conditions were used for both templates, setting the annealing temperature according to the template (60°C for ITS- specific PCR primers). Difficult

templates and repeated regions were solved by increasing initial denaturation time and modifying thermal cycling conditions as follows: 40 cycles of denaturation at 96°C for 10 s and annealing/ extension at 50°C for 4 min. The *Chaetoceros* spp. and *Skeletonema* spp. 18S rDNA sequences were aligned *in silico* using the BLAST database.

Statistical analyses

A logistic model was fitted to *C. socialis* and *S. marinoi* growth curves generated by considering both abundance and chl *a* estimations. Data fitting with the model was evaluated by the root mean square error (RMSE) and r^2. To evaluate relationships between the considered variables, Spearman's rank correlation was computed. All statistical analyses were performed with PAST ver. 4.01 (Hammer et al., 2001).

RESULTS

Sequence analyses

The 18S rDNA amplicons of *C. socialis* CBA22 (GenBank accession no. OQ630515) and *S. marinoi* CBA4 (GenBank accession no. OQ630516), obtained by qPCR amplification using new developed primers, were sequenced and results confirmed (i) the correct alignment with target sequences for DNA and cDNA in BLAST database (www. https://blast.ncbi.nlm.nih.gov) and (ii) the expected amplicon size of 132 and 118 bp, respectively. The primers targeting *Chaetoceros* spp. and *Skeletonema* spp. resulted genus specific.

Standard curve characterization

Standard curves for the different target diatom taxa were generated using either DNA or cDNA. For the 18S rDNA diatom target, previous characterized standard curves were used (Casabianca et al., 2021), while for *Chaetoceros* spp. and *Skeletonema* spp. primers different standard curves were obtained. In particular, when DNA was amplified in qPCR, the mean standard curves for *Chaetoceros* spp. and *Skeletonema* spp. primers, showed a PCR efficiency of 99 and 100% (mean standard curves: y = - 3.35x + 23.25 and y = - 3.32x + 18.14 for *Chaetoceros* spp. and *Skeletonema* spp., respectively) and a linear relationship over six orders of magnitude (r^2 = 0.99). When cDNA was used as a template, the mean standard curves for *Chaetoceros* spp. and *Skeletonema* spp. showed a PCR efficiency of 98 and 100%, respectively (mean standard curves: y = -3.37x+ 17.37 and y = -3.33x + 12.5 for *Chaetoceros* spp. and *Skeletonema* spp., respectively) and a linear relationship over six orders of magnitude (r^2 = 0.99). The slopes obtained by the standard curves were used for calculation of diatom, *Chaetoceros* spp. and *Skeletonema* spp. 18S rRNA/rDNA ratios as reported in Casabianca et al. (2021).

Individual species *C. socialis* and *S. marinoi* growth experiments: biomass relationships and variations, and changes in RNA/DNA ratios

Biomass expressed as cell abundance, chl *a*, cellular carbon content, and various molecular variables, such as *C. socialis* and *S. marinoi* RNA/DNA ratios, taxon specific amplified *Chaetoceros* spp. and *Skeletonema* spp. 18S rRNA/rDNA ratios, and total protein contents were analyzed in cultured growing systems (Table I).

In order to test the degree of association between cell abundance, biomass estimation expressed as chl *a*, cellular carbon and protein content and to assess whether these variables showed a direct proportionality or a non linear monotonic correlation, Spearman's rank correlations for *C. socialis* (Fig. 1A) and *S. marinoi* (Fig. 1B) were applied. Significant positive correlations between the analysed variables for both species were found.

The logistic model fitted growth curves obtained by cell abundance and chl *a* estimation for both diatom species and the inflection points of the cell curves, representing the most rapid growth were reached after 6 and 8 days with abundance of 4.7 x 10^5 cells mL^{-1} (corresponding to 136.0 μg mL^{-1} of chl *a*) and 4.0 x 10^5 cells mL^{-1} (corresponding to 210.8 μg mL^{-1} of chl *a*) for *C. socialis* CBA22 and *S. marinoi* CBA4, respectively (Fig. 2 A and B). The *C. socialis* logistic growth rates were 0.53 and 0.29 day^{-1} obtained by cell abundance and chl *a* content, respectively, within 4 - 8 day range. Considering the same day range, the logistic growth rates for *S. marinoi* CBA4 were 0.39 and 0.42 day^{-1} by cell abundance and chl *a*, respectively. The model stationary growth phase showed maximum cell abundance of 6.5 x 10^5 and 7.1 x 10^5 cells mL^{-1} for *C. socialis* CBA22 and *S. marinoi* CBA4, respectively (Fig. 2). A similar trend for both taxa was obtained by chl *a* estimations with model chl *a* values of 318.6 and 395.6 μg L^{-1} for *C. socialis* CBA22 and *S. marinoi* CBA4, respectively.

The estimations of RNA/DNA ratios obtained by total nucleic acid concentrations and taxon specific *Chaetoceros* and *Skeletonema* 18S rRNA/rDNA ratios, were obtained during the entire growth phase of the target species. The RNA/DNA ratios showed maximum values at 2 and 6 days before the two diatom respective exponential growth phases corresponding to 23.2 ± 1.5 and 15.3 ± 0.8 for *C. socialis* CBA22 and *S. marinoi* CBA4, respectively. Similar results were obtained for the 18S rRNA/rDNA ratio using primers targeting the *Chaetoceros* spp. and *Skeletonema* spp. Maximum values were obtained at 2 and 6 days before exponential growth phases of both diatoms, corresponding to 16.2 ± 1.6 and 30.1 ± 5.4 for *C. socialis* CBA22 and *S. marinoi* CBA4, respectively. The two diatom growth curves fitted the logistic curve model, while the RNA/DNA and 18S rRNA/rDNA ratios for the target taxa considered reached the maximum values at the early stage of the growth curve, right prior to its steepest section.

Co-cultured *C. socialis* and *S. marinoi* growth experiments: biomass relationships and variations, and changes in RNA/DNA ratios

A second experimental setup included the study of biomass and RNA/DNA ratio variations in a mixture of the two species, *C. socialis* and *S. marinoi*, culture system. The same variables analysed in individual culture systems were examined (Table II).

In co-culture experiments, the degree of association and the existence of proportionality between cell abundance, chl *a*, cellular carbon and protein content and to assess whether these variables showed a direct proportionality or a non linear monotonic correlation, were also tested by Spearman's rank correlations (Fig. 3). Even within these systems, all the variables were highly correlated.

The exponential phase of the co-culture species was reached later than individual species culture experiments. The maximum total cell abundance of $4.6 \times 10^6 \pm 2.7 \times 10^3$ cells mL^{-1} was achieved at the end of growth curves (Fig. 4A) and corresponded to $2.1 \times 10^3 \pm 8.7 \times 10^1$ μg L^{-1} of the chl *a* (Fig. 4B). The total RNA/DNA (Fig. 4C) and diatom 18S rRNA/rDNA (Fig. 4D) ratios showed maximum values of 13.4 ± 0.4 and 9.4 ± 0.7, respectively, 4 days later than the initial inoculum at the early stage of the growth curve as observed in experiments on individual species. Cell abundance of *C. socialis* reached a maximum value of $4.3 \times 10^6 \pm 5.2 \times 10^3$ cells mL^{-1} (Fig. 5A) by the end of the stationary phase while *S. marinoi* reached its maximum cell density of $6.6 \times 10^5 \pm 2.9 \times 10^3$ cells mL^{-1} on 18th day of growth curve (Fig. 5B). Also in the co-culture experiment, molecular ratios for each target taxon were applied to estimate metabolic variations. In particular, *Chaetoceros* and *Skeletonema* 18S rRNA/rDNA ratios were evaluated throughout the growth phase and maximum values of 24.4 ± 2.0 and 8.2 ± 0.7, respectively, were observed 4 days after the initial inoculum for both species.

DISCUSSION

In this study, the two diatom species *Chaetoceros socialis* and *Skeletonema marinoi,* which both dominate seasonal recurrent winter–spring blooms in Northwestern Adriatic Sea, were used for biomass growth and metabolic activity investigation either in individual and co-culture experiments. Cell abundance and biomass estimation, expressed as chl *a*, cellular carbon and protein contents showed significant positive correlations confirming that all variables were linearly related. Further, a logistic model was used to describe the target diatoms' growth curve of both diatom species generated by abundance and chl *a* concentration. These growth curves fitted well the logistic curve model, which divided growth into a slow initial phase, followed by an increase in cell abundance, and then stationary phase characterized by constant cell concentration. These variables

can describe both biomass and growth dynamic, but they were not able to provide information on metabolic activity of phytoplanktonic cells. Total RNA/DNA and taxon specific 18S rRNA/rDNA ratios of *C. socialis* and *S. marinoi* were analysed. Individual *C. socialis* and *S. marinoi* 18S rRNA/rDNA ratios were significantly correlated with their respective RNA/DNA ratios obtained by nucleic acid concentrations ($r_s = 0.420$, $P < 0.01$ and $r_s = 0.404$, $P < 0.01$ for *C. socialis* and *S. marinoi,* respectively), and both ratio values for the two species showed different maximum values at the beginning of the growth curve. These high values were observed at 2 and 6 days in the lag phase of growth for *C. socialis* and *S. marinoi*, respectively, probably depending on species-specific metabolic pathways which depend on different conditions, such as resources or light availability (Chícharo and Chícharo, 2008; Cross et al., 2015; Marañón et al., 2018). These values decreased significantly in exponential phase of growth remaining at low levels throughout the stationary phase and showing an opposite trend to the increasing diatom abundance and biomass. This opposite trend between RNA/DNA molecular ratio variations and biomass dynamic was also demonstrated by significant negative correlations between molecular ratios and growth variables of abundance, chl *a*, carbon content and proteins (from $r_s = -0.678$ to $r_s = -0.566$, $P < 0.001$, for both species). For decades, RNA/DNA ratios have been used as an indicator of growth in various marine organisms also including phytoplankton on field (Dortch et al., 1983; Dortch et al., 1985; Clarke et al., 1988; Mordy and Carlson, 1991; Casabianca et al., 2021). RNA is associated with protein synthesis, and specifically rRNA (ribosomal RNA) is an important component of ribosomes, which are required for protein synthesis (Blazewicz et al., 2013; Toseland et al., 2013; Finkel et al., 2016). The RNA and rRNA variable cellular concentration are associated with transcriptional and translational levels, and, assuming that DNA amount is stable, the RNA/DNA ratio increases with protein synthesis demand and then with metabolic activity increments during active growth (Chícharo and Chícharo, 2008; Blazewicz et al., 2013). Since the RNA abundance is correlated with protein synthesis, high RNA/DNA ratio reflected an increased gene expression per cell being an approximation for gene expression levels (Wemheuer et al., 2015). The use of these molecular ratios could be useful to identify metabolism activation occurring in the first stages of growth. In previous studies, relationships between higher RNA/DNA ratio, which may provide an estimate of nutritional condition and protein synthesis, and higher metabolic activity in favor of growth has been suggested (García et al., 1998; Buckley et al., 1999; Humphrey et al., 2007; Delegrange et al., 2015). The higher molecular RNA/DNA and 18S rRNA/rDNA ratios observed in this study for both diatom species during the lag phase may be explained by higher active metabolism of cells maintained in appropriate experimental conditions of temperature, light irradiance, and nutrient supply, which can allow cells to grow according to the standard logistic growth model (Olson et al.,

1986; Kemp et al., 1993; Poulsen et al., 1993; Flynn et al., 2010; Blazewicz et al., 2013; Daines et al., 2014).

Also, in co-culture experiments of *C. socialis* and *S. marinoi*, all the variables of biomass variation exhibited significant positive correlations. The maximum values of abundance, biomass and molecular ratios occurred in different growth phases as it was clearly observed, and proved by significant negative correlations between total RNA/DNA, diatom 18S rRNA/rDNA and diatom abundance (r_s = -0.887, $P < 0.001$; r_s = -0.758, $P < 0.001$, for total RNA/DNA and diatom 18S rRNA/rDNA, respectively) and biomass as chl *a* (r_s = -0.891, $P < 0.001$; r_s = -0.761, $P < 0.001$, for total RNA/DNA and diatom 18S rRNA/rDNA, respectively). The maximum molecular ratio values were obtained in the lag phase (4th day) of both diatom growth, whereas the highest abundance and biomass values were reported in the late exponential growth phase. It was likely that rRNA (which accounts for around 80% of total RNAs in a cell for translation, along with ribosomal proteins) was required prior for the translation activity and subsequent biosynthetic activation for cellular growth (Neidhardt, 1987; Campbell et al., 2011; Blazewicz et al. 2013; Toseland et al., 2013). Further, more qualitative approaches used rRNA to detect currently active microbial populations. In general, it is considered that RNA is not always significantly correlated with growth rate, but that the heterogeneity of metabolic activity, life history, life strategy, nutrient availability and environmental factors can modulate the rRNA activity in relation to the microbial population growth rate (Mitchell et al., 2009; Sukenik et al., 2012).

In the current study, total culture biomass was dominated by *C. socialis* during the active growth phase of both diatoms under constant nutrient supply, outcompeting *S. marinoi*, which was growing at low cellular concentrations throughout the entire growth curve until the 18th day, followed by a decrease with respect to *C. socialis*, which increased due to the apparently different nutrient requirements (Tilman et al., 1981). It was also known that under nutrient availability, changes in phytoplankton species composition might occur by shifting the species interactions from nutrients to other resources competition (Tilman et al., 1985; Burson et al., 2018).

In co-culture experiments, as well as in individual culture system, the diatom growth was determined by cell abundance, chl *a*, cellular carbon and protein content. Meanwhile, functional metabolic responses were provided by taxon specific 18S rRNA/rDNA ratios of *C. socialis* and *S. marinoi*. A significant decrease of the taxon specific molecular ratios, starting from the exponential phase, was observed with an opposing trend respect to species-specific abundance as demonstrated by significant negative correlations (r_s = -0.760, $P < 0.001$ and r_s = -0.604, $P < 0.001$, for *C. socialis* and *S. marinoi*, respectively). An increase of 1.5 fold and a reduction of 4 fold in 18S rRNA/rDNA ratio were observed for *C. socialis* and *S. marinoi,* respectively, than when species were grown individually. The *C. socialis* 18S rRNA/rDNA ratio showed decreased rapidly right

after the maximum, while the *S. marinoi* 18S rRNA/rDNA ratio displayed a less pronounced decline, most likely due to metabolic activity associated with lower abundance with respect to *C. socialis*. In the current study, this outcome may reflect an interspecific interaction between *C. socialis* and *S. marinoi* as also shown by their differing biomass patterns (Tilman et al., 1981; Elser et al., 2010; Bestion et al., 2018). According to these findings, the taxon-specific molecular ratios developed on target 18S rDNA subunits may express metabolic activity variation during diatom growth phases and they can provide information about the metabolic state of individual phytoplankton species or when they were also grown together. Specifically, molecular ratios may be used for assessing degrees of metabolic/functional activation during the early stages of algal species growth, but only after extensive field validation. Then, the taxon specific 18S rRNA/rDNA ratios can be applied to target species within assemblages to determine whether one species has higher levels of metabolic activation than others, and it is expected that it will grow at higher biomass.

Furthermore, within phytoplankton assemblages, RNA/DNA or 18S rRNA/rDNA molecular ratios were significantly correlated with RNA variability, potentially reflecting changes in metabolic phytoplanktonic cellular activity and linking to biomass growth and protein synthesis (Pommier et al., 2010; Casabianca et al., 2021; Lin et al., 2018). As a result, after field confirmation, the taxon-specific 18S rRNA/rDNA ratio should be employed as a specific and relative indicator of the functional biomass dynamic of species or groups within phytoplankton assemblages. In particular, the study of these molecular ratios in high frequency of sampling should be performed in semi-enclosed areas, to avoid phytoplankton assemblages' replacement and variation due to currents in coastal waters, as occurs in Northwestern Adriatic Sea under Western Adriatic Current (WAC) and seasonal phytoplankton succession (Totti et al., 2019; Grilli et al., 2020; Casabianca et al., 2021; Neri et al., 2023). In this study, the use of *Skeletonema* spp. primers for the potentially estimation of 18S rRNA/rDNA ratio in the NW Adriatic Sea resulted specific also for diatoms *Detonula* spp. and *Thalassiosira* spp. as high homology sequence and partially unresolved phylogenetic positions of these taxa (Kaczmarska et al., 2005; Hoppenrath et al., 2007). In any case, the first taxon was infrequently identified in Adriatic seawater samples, whilst the latter was discovered to be present in low abundance percentages ranging from 0.04 to 10% in comparison to *Skeletonema* spp. (Totti et al., 2019; Casabianca et al., 2021) (data not shown). Therefore, the use of *Skeletonema* primers can be justified in this preliminary study on the application of taxon specific 18S rRNA/rDNA ratio.

CONCLUSIONS

In this study, RNA/DNA and taxon-specific 18S rRNA/rDNA ratios were examined throughout the growth phases of two diatom species' individual and co-culture systems. The molecular variable

dynamic indicated that the variations were linked to changes in metabolic activity, whereas biomass measured by cell abundance, chl *a*, or carbon content was able to describe growth trends of *C. socialis* and *S. marinoi*. In this preliminary study, taxon-specific 18S rRNA/rDNA ratio may indicate the cellular metabolism activation prior to target algal species high rate of replication, and then, expects high biomass proliferation potentially representing a predictive tool of phytoplankton assemblage dynamics in coastal waters in the future.

ACKNOWLEDGEMENTS

We thank Dr. Nadia Marinchel and Dr. Francesca Ottaviani for their help in the experimental setup and Dr. Aurora Diotallevi for PCR products sequencing.

FUNDING

This study has received funding from the EU Interreg Italy-Croatia WATERCARE Project (Water management solutions for reducing microbial environment impact in coastal areas - Grant 10044130) and from University of Urbino (Department of Bimolecular Sciences -Grant DISB_PENNA_PRIN09).

REFERENCES

Berdalet, E., Roldan, C., Olivar, M. P. and Lysnes, K. (2005) Quantifying RNA and DNA in planktonic organisms with SYBR Green II and nucleases Part A. Optimisation of the assay. *Sci. Mar.*, **69**, 1–16.

Bernardi Aubry, F., Berton, A., Bastianini, M., Socal, G. and Acri, F. (2004) Phytoplankton succession in a coastal area of the NW Adriatic, over a 10-year sampling period (1990–1999). *Cont. Shelf Res.*, 24, 97–115.

Bestion, E., García-Carreras, B., Schaum, C. E., Pawar, S. and Yvon-Durocher, G. (2018) Metabolic traits predict the effects of warming on phytoplankton competition. *Ecol. Lett.*, **21**, 655–664.

Blazewicz, S. J., Barnard, R. L., Daly, R. A. and Firestone, M. K. (2013) Evaluating rRNA as an indicator of microbial activity in environmental communities: limitations and uses. *ISME J.* **7**, 2061–2068.

Brett, M. T., Kainz, M. J., Taipale, S. J. and Seshan, H. (2009) Phytoplankton, not allochthonous carbon, sustains herbivorous zooplankton production. *Proc. Natl. Acad. Sci. USA*, **106**, 21197–21201.

Buckley, L., Caldarone, E. and Ong, T. L. (1999) RNA–DNA ratio and other nucleic acid-based indicators for growth and condition of marine fishes. *Hydrobiologia*, **401**, 265–277.

Burson, A., Stomp, M., Greenwell, E., Grosse, J. and Huisman, J. (2018) Competition for nutrients and light: testing advances in resource competition with a natural phytoplankton community. *Ecology*, **99**, 1108–1118.

Cabrini, M., Fornasaro, D., Cossarini, G., Lipizer, M. and Virgilio, D. (2012) Phytoplankton temporal changes in a coastal northern Adriatic site during the last 25 years. *Estuar. Coast Shelf Sci.*, **115**, 113-124.

Campbell, B. J., Yu, L., Heidelberg, J. F. and Kirchman, D. L. (2011) Activity of abundant and rare bacteria in a coastal ocean. *Proc. Natl. Acad. Sci. USA*, **108**, 12776–12781.

Casabianca, S., Capellacci, S., Ricci, F., Scardi, M,. and Penna, A. (2021) Phytoplankton RNA/DNA and 18S rRNA/rDNA ratios in a coastal marine ecosystem *J. Plankton Res.*, **43**, 367-379.

Casabianca, S., Capellacci, S., Ricci, F., Scardi, M. and Penna, A. (2022) A phytoplankton time series in the Northwestern Adriatic Sea: Structure and dynamics of the assemblages in a coastal ecosystem. *Estuar. Coast. Shelf Sci.*, **278**, 108109.

Chavez, F. P., Messié, M. and Pennington, J. T. (2011) Marine primary production in relation to climate variability and change. *Annu. Rev. Mar. Sci.*, **3**, 227–260.

Chícharo, M. A. and Chícharo, L. (2008) RNA:DNA ratio and other nucleic acid derived indices in marine ecology. *Int. J. Mol. Sci.*, **9**, 1453–1471.

Clarke, A., Rodhouse, P. G., Holmes, L. J. and Pascoe, P. L. (1988) Growth rate and nucleic acid ratio in cultured cuttlefish *Sepia officinalis* (Mollusca: Cephalopoda). *J. Exp. Mar. Biol. Ecol.*, **133**, 229-240.

Cross, W. F., Hood, J. M., Benstead, J. P., Huryn, A. D. and Nelson, D. (2015) Interactions between temperature and nutrients across levels of ecological organization. *Glob. Change Biol.*, **21**, 1025–1040.

Daines, S. J., Clark, J. R. and Lenton, T. M. (2014) Multiple environmental controls on phytoplankton growth strategies determine adaptive responses of the N:P ratio. *Ecol. Lett.*, **17**, 414-425.

Delegrange, A., Vincent, D., Duret, M. and Amara R. (2015) The use of mussels for mitigating the noxious effect of phytoplankton spring blooms on farmed fish. *Aquac. Eng.*, **66**, 52–61

Dortch, Q., Clayton, J. R., Thoresen, S. S., Cleveland, J. S., Bressler, S. L. and Ahmed, S. I. (1985) Nitrogen storage and use of biochemical indices to assess nitrogen deficiency and growth rate in natural plankton populations. *J. Mar. Res.*, **43**, 437-464.

Dortch, Q., Roberts, T. L., Clayton, J. R. and Ahmed, S. I. (1983) RNA/DNA ratios and DNA concentrations as indicators of growth rate and biomass in planktonic organisms. *Mar. Ecol. Prog. Ser.*, **13**, 61–71.

Elser, J. J., Fagan, W. F., Kerkhoff, A. J., Swenson, N. G. and Enquist, B. J. (2010) Biological stoichiometry of plant production: Metabolism, scaling and ecological response to global change. *New Phytol.*, **186**, 593–608.

Falkowski, P. G. (2002) The ocean's invisible forest. *Sci. Am.*, **287**, 38-45.

Finkel, Z.V., Follows, M. J. and Irwin, A. J. (2016) Size-scaling of macromolecules and chemical energy content in the eukaryotic microalgae. *J. Plankton Res.*, **38**, 1151–1162.

Flynn, K. J., Raven, J. A., Rees, T. A. V., Finkel, Z. V., Quigg, A. and Beardall, J. (2010) Is the growth rate hypothesis applicable to microalgae? *J. Phycol.*, **46**, 1–12.

Follows, M. J. and Dutkiewicz, S. (2011) Modeling diverse communities of marine microbes. *Ann. Rev. Mar. Sci.*, **3**, 427-51.

García, A., Cortés, D. and Ramírez, T. (1998) Daily larval growth and RNA and DNA contents of the NW Mediterranean anchovy *Engraulis encrasicolus* and their relations to the environment. *Mar. Ecol. Prog. Ser.*, 166, 237-245.

Garcia, N. S., Bonachela, J. A. and Martiny, A. C. (2016) Interactions between growth-dependent changes in cell size, nutrient supply and cellular elemental stoichiometry of marine *Synechococcus*. *ISME J.*, **10**, 2715-2724.

Grilli, F., Accoroni, S., Acri, F., Bernardi Aubry, F., Bergami, C., Cabrini, M., Campanelli, A., Giani, M. *et al.* (2020) Seasonal and interannual trends of oceanographic parameters over 40 Years in the Northern Adriatic Sea in relation to nutrient loadings using the EMODnet chemistry data portal. *Water*, **12**, 2280.

Guillard, R. R. L. (1975) Culture of phytoplankton for feeding marine invertebrates. In: Smith, W. L. and Chanley MH (eds.), *Culture of marine invertebrate animals.* Plenum Press, New York, pp. 26–60.

Hammer, Ø., Harper, D. A. T. and Ryan, P. D. (2001) PAST: Paleontological statistics software package for education and data analysis. *Palaeontol. Electron.*, **4**, art4. https://palaeo-electronica.org/2001_1/past/past.pdf.

Holm-Hansen, O., Lorenzen, C. J., Holmes, R. W. and Strickland, J. D. H. (1965) Fluorimetric determination of chlorophyll. *J. Cons. Int. Explor. Mer.*, **30**, 3-15.

Hoppenrath, M., Beszteri, B., Drebes, G., Halliger, H., Beusekom, J. E. E., Janisch, S. and Wiltshire, K. H. (2007). *Thalassiosira species* (Bacillariophyceae, Thalassiosirales) in the North Sea at Helgoland (German Bight) and Sylt (North Frisian Wadden Sea) - a first approach to assessing diversity. *Eur. J. Phycol.*, **42**, 271–288.

Humphrey, C.A., King, S.C. and Klumpp, D.W. (2007) A multibiomarker approach in barramundi (*Lates calcarifer*) to measure exposure to contaminants in estuaries of tropical North Queensland. *Mar. Pollut. Bull.*, **54**, 1569-1581.

Ikeda, T., San, F., Yamaguchi, A. and Matsuishi, T. (2007) RNA:DNA ratios of calanoid copepods from the epipelagic through abyssopelagic zones of the North Pacific Ocean. *Aquatic. Biol.*, **1**, 99–108.

Kaczmarska, I., Beaton, M., Benoit, A.C. and Medlin, L.K. (2005) Molecular phylogeny of selected members of the order Thalassiosirales (Bacillariophyta) and evolution of the fultoportula. *J. Phycol.*, **42**, 121–138.

Kemp, P., Lee, S. and LaRoche, J. (1993) Estimating the growth rate of slowly growing marine bacteria from RNA content. *Appl. Environ. Microbiol.*, **59**, 2594.

Kruk, C. V., Huszar, L. M., Peeters, E., Bonilla, S., Costa, L., Lurling, M., Reynolds, C. S. and Scheffer M (2010) A morphological classification capturing functional variation in phytoplankton. *Freshw. Biol.*, **55**, 614–627.

Larkin, M. A., Blackshields, G., Brown, N. P., Chenna, R., McGettigan, P. A., McWilliam, H., Valentin, F., Wallace, I. M. *et al.* (2007) Clustal W and Clustal X version 2.0. *Bioinformatics*, **23**, 2947−2948.

LeGresley, M. and McDermott, G. (2010) Counting chamber methods for quantitative phytoplankton analysis - haemocytometer, Palmer- Maloney cell and Sedgewick-Rafter cell. In: Karlson, B., Cusack, C. and Bresnan, E. (eds.), *Microscopic and Molecular Methods for Quantitative Phytoplankton Analysis.* UNESCO, Paris, pp. 25−30.

Lin, Y. C., Kang, L. K., Shih, C. Y., Gong, G. C. and Chang, J. (2018) Evaluation of the relationship between the 18S rRNA/rDNA ratio and population growth in the marine diatom *Skeletonema tropicum* via the application of an exogenous nucleic acid standard. *J. Eukaryot. Microbiol.*, **65**, 792–803.

Litchman, E. and Klausmeier, C. A. (2008) Trait-based community ecology of phytoplankton. *Ann. Rev. Ecol. Evol. Syst.*, **39**, 615–639.

Litchman, E., Klausmeier, C. A., Schofield, O. M. and Falkowski, P. G. (2007) The role of functional traits and trade-offs in structuring phytoplankton communities: Scaling from cellular to ecosystem level. *Ecol. Lett.*, **10**, 1170–1181.

Loladze, I. and Elser, J. J. (2011) The origins of the Redfield nitrogen-to-phosphorus ratio are in a homoeostatic protein to rRNA ratio. *Ecol. Lett.*, **14**, 244–250.

Mangoni, O., Basset, A., Bergamasco, A., Carrada, G. C., Margiotta, F., Passarelli, A., Rivaro, P., Saggiomo, M. *et al.* (2013) A case study on the application of the MSFD to Mediterranean coastal systems: the Po plume, as a transitional water system in the Northern Adriatic basin. *Trans. Waters Bull.*, 7, 175–201.

Mangoni, O., Modigh, M., Mozetič, P., Bergamasco, A., Rivaro, P. and Saggiomo, V. (2008) Structure and photosynthetic properties of phytoplankton assemblages in a highly dynamic system, the Northern Adriatic Sea. *Estuar. Coast. Shelf Sci.*, 77, 633–644.

Marañón, E., Cermeno, P., Latasa, M. and Tadonléké, R. D. (2012) Temperature, resources, and phytoplankton size structure in the ocean. *Limnol. Oceanogr.*, **67**, 1266-1278.

Marañón, E., Lorenzo, M. P., Cermeño, P., and Mouriño-Carballido, B. (2018) Nutrient limitation suppresses the temperature dependence of phytoplankton metabolic rates. *ISME J.*, **12**, 1836–1845.

Marra, J. (2009) Net and gross productivity: weighing in with ^{14}C. *Microb. Ecol.*, **56**, 123–131.

Menden-Deuer, S. and Lessard, E. J. (2000) Carbon to volume relation- ships for dinoflagellates, diatoms, and other protist plankton. *Limnol. Oceanogr.*, **45**, 569–579.

Mitchell, A,. Romano, G. H., Groisman, B., Yona, A., Dekel, E., Kupiec, M., Dahan, O. and Pilpel, Y. (2009) Adaptive prediction of environmental changes by microorganisms. *Nature*, **460**: 220–224.

Mordy, C. W. and Carlson, D. J. (1991) An evaluation of fluorescence techniques for measuring DNA and FWA in marine microorganisms. *Mar. Ecol. Prog. Ser.*, **73**, 283–93.

Naselli-Flores, L. and Barone, R. (2011) Fight on plankton! Or, phytoplankton shape and size as adaptive tools to get ahead in the struggle for life. *Cryptog. Algol.*, **32**, 157–204.

Neidhardt, F. C. (1987) Chemical composition of *Escherichia coli*. In: Neidhardt, F. C., Ingraham, J. L., Low, K. B., Magasanik, B., Schaechter, M. and Umbarger, H. E. (eds), Escherichia coli *and* Salmonella typhimurium: *Cellular and Molecular Biology*. American Society for Microbiology; Washington, DC.

Nejstgaard, J. C., Frischer, M. E., Raule, C. L., Gruebel, R., Kohlberg, K. E. and Verity, P. G. (2003) Molecular detection of algal prey in copepod guts and faecal pellets. Limnol. Oceanogr., *Methods*, **1**, 29–38.

Neri, F., Romagnoli, T., Accoroni, S., Ubaldi, M., Garzia, A., Pizzuti, A., Campanelli, A., Grilli, F. *et al.* (2023) Phytoplankton communities in coastal and offshore stations of the northern Adriatic Sea approached by network analysis and different statistical descriptors. *Estuar. Coast. Shelf S.*, 108224.

Nicklisch, A. and Steinberg CEW (2009) RNA/protein and RNA/DNA ratios determined by flow cytometry and their relationship to growth limitation of selected planktonic algae in culture. *Eur. J. Phycol.*, **44**, 297–308.

Olson, R., Vaulot, D. and Chisholm, D. (1986) Effects of environmental stresses on the cell cycle of two marine phytoplankton species. *Plant. Physiol.*, **80**, 918-925.

Penna, A., Casabianca, S., Perini, F., Bastianini, M., Riccardi, E., Pigozzi, S. and Scardi, M. (2013) Toxic *Pseudo-nitzschia* spp. in the northwestern Adriatic Sea: characterization of species composition by genetic and molecular quantitative analyses. *J. Plankton Res.*, **35**, 352–366.

Penna, N., Capellacci, S. and Ricci, F. (2004) The influence of the Po River discharge on phytoplankton bloom dynamics along the coastline of Pesaro (Italy) in the Adriatic Sea. *Mar. Pollut. Bull.*, **48**, 321–326.

Perini, F., Bastianini, M., Capellacci, S., Pugliese, L., DiPoi, E., Cabrini, M., Buratti, S., Marini, M. *et al.* (2019) Molecular methods for cost-efficient monitoring of HAB (harmful algal bloom) dinoflagellate resting cysts. *Mar. Pollut. Bull.*, **147**, 209−218.

Pommier, J., Frenette, J. J. and Glemet, H. (2010) Relating RNA:DNA ratio in *Eurytemora affinis* to seston fatty acids in a highly dynamic environment. *Mar. Ecol. Prog. Ser.*, **400**, 143–154.

Poulsen, L., Ballard, G. and Stahl, D. (1993) Use of rRNA fluorescence in situ hybridization for measuring the activity of single cells in young and established biofilms. *Appl. Environ. Microbiol.*, **59**, 1354.

Ricci, F., Capellacci, S., Campanelli, A., Grilli, F., Marini, M. and Penna, A. (2022) Long-term dynamics of annual and seasonal physical and biogeochemical properties: role of minor river discharges in the North-western Adriatic coast. *Estuar. Coast. Shelf. Sci.*, **272**, 107902

Roselli, L. and Basset, A. (2015) Decoding size distribution patterns in marine and transitional water phytoplankton: from community to species level. *PLOS ONE*, **10**, e0127193.

Socal, G., Acri, F., Bastianini, M., Bernardi Aubry, F., Bianchi, F., Cassin, D., Coppola, J., De Lazzari, A. *et al.* (2008) Hydrological and biogeochemical features of the Northern Adriatic Sea in the period 2003–2006. *Mar. Ecol.*, **29**, 449–468.

Strickland, J. D. H. and Parsons, T. R. (1972) A Practical Handbook of Seawater Analysis. 2nd ed Fisheries Research Board of Canada Ottawa, Canada.

Sukenik, A., Kaplan-Levy, R. N., Welch, J. M. and Post, A. F. (2012). Massive multiplication of genome and ribosomes in dormant cells (akinetes) of *Aphanizomenon ovalisporum* (Cyanobacteria). *ISME J.*, **6**, 670–679.

Tilman, D. (1985) The resource-ratio hypothesis of plant succession. *Am. Nat.*, **125**, 827-852.

Tilman, D., Mattson, M. and Langer, S. (1981) Competition and nutrient kinetics along a temperature gradient: an experimental test of a mechanistic approach to niche theory. *Limnol. Oceanogr.*, **26**, 1020–1033.

Toseland, A., Daines, S. J., Clark, J. R., Kirkham, A., Strauss, J., Uhlig, C., Lenton, T. M., Valentin, K. *et al.* (2013) The impact of temperature on marine phytoplankton resource allocation and metabolism. *Nature Clim. Change*, **3**, 979–984.

591 Totti, C., Romagnoli, T., Accoroni, S., Coluccelli, A., Pellegrini, M., Campanelli, A., Grilli, F. and
592 Marini, M. (2019) Phytoplankton communities in the northwestern Adriatic Sea:
593 interdecadal variability over a 30-years period (1988 – 2016) and relationships with
594 meteoclimatic drivers. *J. Mar. Syst.*, **193**, 137–153.
595 Wemheuer, B., Wemheuer, F., Hollensteiner, J., Meyer. F. D., Voget, S. and Daniel, R. (2015) The
596 green impact: bacterioplankton response towards a phytoplankton spring bloom in the
597 southern North Sea assessed by comparative metagenomic and metatranscriptomic
598 approaches. *Front. Microbiol*., **6**, 805.
599 Wood, A. M., Everroad, R. C. and Wingard, L. M. (2005) Measuring growth rates in microalgal
600 cultures. In: Anderson, R. A. (ed.), *Algal Culturing Techniques*. Elsevier Academic Press,
601 London, pp. 269–286.
602 Ye, J., Coulouris, G., Zaretskaya, I., Cutcutache, I., Rozen, S. and Madden, T. L. (2012) Primer-
603 BLAST: a tool to design target specific primers for polymerase chain reaction. *BMC*
604 *Bioinformatics*, **13**, 134.
605 Yentsch, C. S. and Menzel, D. W. (1963) A method for the determination of phytoplankton
606 chlorophyll and phaeophytine by fluorescence. *Deep Sea Res.*, **10**, 221-231.
607

608 Table and Figure legends
609
610 Table I: Biomass expressed as abundance (cells mL^{-1}), chl *a* ($\mu g\ L^{-1}$), carbon content (mg C L^{-1}),
611 and molecular variables as RNA/DNA ratio, taxon specific 18S rRNA/rDNA ratio for *C. socialis*
612 and *S. marinoi*, and total proteins (mg L^{-1}) obtained during the entire growth phase of *C. socialis*
613 CBA22 and *S. marinoi* CBA4 in this study.
614
615 Table II: Biomass expressed as chl *a* ($\mu g\ L^{-1}$), carbon content (mg C L^{-1}), cell abundance (cells mL^{-1})
616 and molecular variables as total diatom RNA/DNA ratio, diatom and taxon specific *Chaetoceros*
617 and *Skeletonema* 18S rRNA/rDNA ratios and total proteins (mg L^{-1}) obtained during the entire
618 growth curve of both *C. socialis* CBA22 and *S. marinoi* CBA4 in co-culture experiments.
619
620 Figure 1. Matrix plot showing bivariate relationships among abundance, chl *a*, carbon content and
621 total proteins as scatterplots for *Chaetoceros socialis* CBA22 (A) and *Skeletonema marinoi* CBA4
622 (B).
623
624 Figure 2. Growth curve of *Chaetoceros socialis* CBA22 (A) and *Skeletonema marinoi* CBA4 (B)
625 expressed as biomass using abundance (cells mL^{-1}) and as chl *a* ($\mu g\ L^{-1}$), and RNA/DNA and taxon
626 specific 18S rRNA/rDNA molecular ratios. Full and dotted red: biomass; blue: RNA/DNA ratio
627 obtained by extracted nucleic acid concentrations; green: *Chaetoceros* and *Skeletonema* 18S
628 rRNA/rDNA ratio. Red dotted line: logistic curve fitted to biomass data. Root mean square error
629 (RMSE) and coefficient of determination (r^2) for abundance and chl *a* were shown, respectively.
630 For each variable, colored areas are delimited by minimum and maximum values. All experiments
631 were conducted in triplicate.
632
633 Figure 3. Matrix plot showing bivariate relationships among abundance, chl *a*, carbon content and
634 total proteins as scatterplots for *Chaetoceros socialis* CBA22 and *Skeletonema marinoi* CBA4 in
635 co-culture experiments.
636
637 Figure 4. Growth curve of *Chaetoceros socialis* CBA22 and *Skeletonema marinoi* CBA4 in co-
638 culture condition analyzed as total biomass using abundance (cells mL^{-1}) (A) and chl *a* ($\mu g\ L^{-1}$)
639 (B), molecular total RNA/DNA (C) and diatom 18S rRNA/rDNA (D) ratios. Circles represented
640 minimum and maximum values for each variable. All experiments were conducted in triplicate.
641

642 Figure 5. Growth curve in mixed cultured conditions analyzed based on abundance (cells mL^{-1}) and
643 molecular ratios of *Chaetoceros socialis* CBA22 (A) and *Skeletonema marinoi* CBA4 (B). Red line
644 represented mean values of abundance (cells mL^{-1}); green line represented mean values of
645 *Chaetoceros* (A) and *Skeletonema* (B) 18S rRNA/rDNA ratio. Triangles and circles represent
646 minimum and maximum values of cell abundance and 18S RNA/DNA ratios, respectively. All
647 experiments were conducted in triplicate.
648
649
650
651

Table I: Biomass expressed as abundance (cells mL^{-1}), chl *a* ($\mu g\ L^{-1}$), carbon content (mg C L^{-1}), and molecular variables as RNA/DNA ratio, taxon specific 18S rRNA/rDNA ratio for *C. socialis* and *S. marinoi*, and total proteins (mg L^{-1}) obtained during the entire growth phase of *C. socialis* CBA22 and *S. marinoi* CBA4 in this study.

Species	Abundance (cells mL^{-1})	Chl *a* ($\mu g\ L^{-1}$)	Carbon content (mg C L^{-1})	RNA/DNA ratio	18S rRNA/rDNA ratio	Total proteins (mg L^{-1})
C. socialis CBA22	$4.0 \times 10^5 \pm 2.6 \times 10^4$	186.8 ± 11.9	6.6 ± 0.4	10.6 ± 0.6	9.2 ± 0.3	15.6 ± 0.9
S. marinoi CBA4	$4.6 \times 10^5 \pm 2.1 \times 10^4$	257.6 ± 12.8	6.7 ± 0.3	6.4 ± 0.3	8.7 ± 0.4	30.2 ± 1.5

Mean ± standard error is reported.

Table II: Biomass expressed as chl *a* (µg L^{-1}), carbon content (mg C L^{-1}), cell abundance (cells mL^{-1}) and molecular variables as total diatom RNA/DNA ratio, diatom and taxon specific *Chaetoceros* and *Skeletonema* 18S rRNA/rDNA ratios and total proteins (mg L^{-1}) obtained during the entire growth curve of both *C. socialis* CBA22 and *S. marinoi* CBA4 in co-culture experiments.

	Mean	Minimum	Maximum
Chl *a* (µg L^{-1})	771.7 ± 69.7	0.1 ± 0.02	$2.1 \times 10^3 \pm 8.7 \times 10^1$
Carbon content (mg C L^{-1})	39.0 ± 3.9	$9.0 \times 10^{-3} \pm 2.8 \times 10^{-4}$	130 ± 19
C. socialis CBA22 abundance (cells mL^{-1})	$1.7 \times 10^6 \pm 1.6 \times 10^5$	250.0 ± 0.2	$4.3 \times 10^6 \pm 5.2 \times 10^3$
S. marinoi CBA4 abundance (cells mL^{-1})	$3.2 \times 10^5 \pm 2.1 \times 10^4$	250.0 ± 0.4	$6.6 \times 10^5 \pm 3.3 \times 10^3$
RNA/DNA ratio	6.8 ± 0.3	2.4 ± 0.1	15.0 ± 0.5
Diatom 18S rRNA/rDNA ratio	5.1 ± 0.2	1.9 ± 0.03	11.8 ± 0.7
Chaetoceros 18S rRNA/rDNA ratio	13.5 ± 0.6	7.6 ± 0.2	31.3 ± 2.0
Skeletonema 18S rRNA/rDNA ratio	5.5 ± 0.1	3.7 ± 0.6	10.7 ± 0.7
Total proteins (mg L^{-1})	113.1 ± 10.2	0.3 ± 0.01	332.1 ± 17.0

Mean ± standard error is reported.

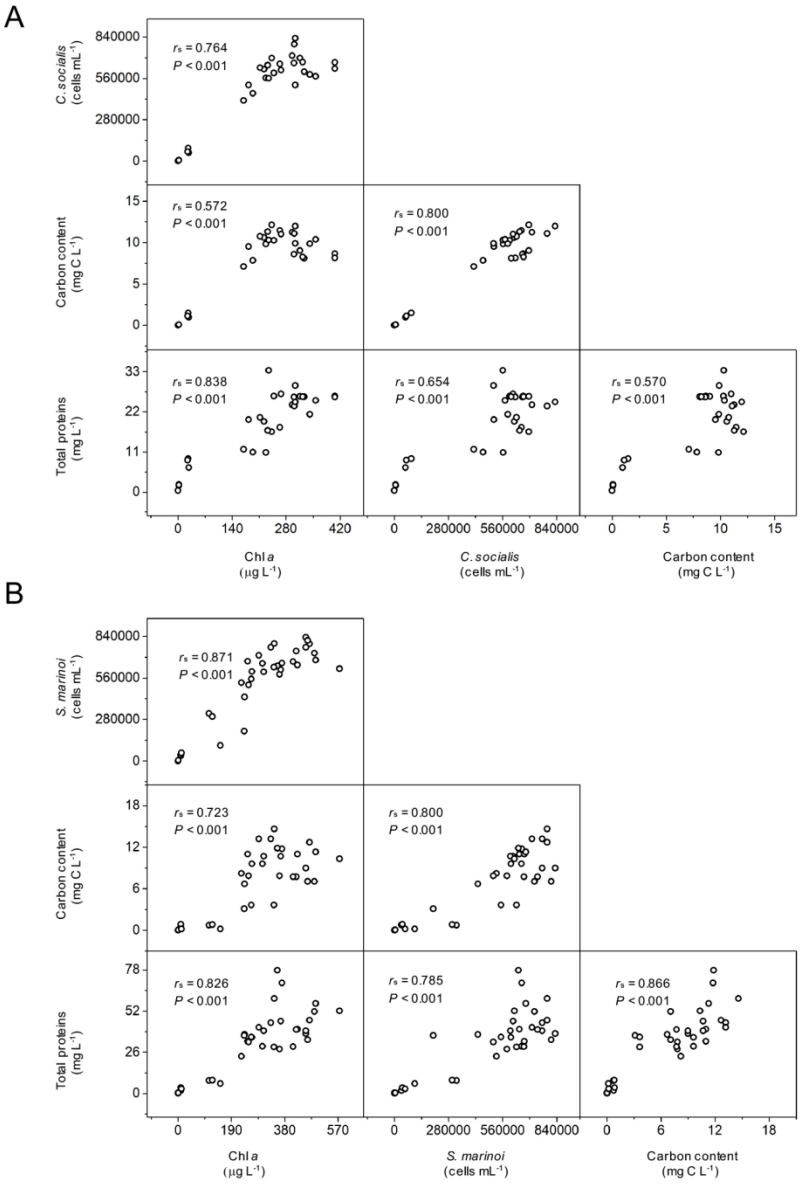

Figure 1. Matrix plot showing bivariate relationships among abundance, chl *a*, carbon content and total proteins as scatterplots for *Chaetoceros socialis* CBA22 (A) and *Skeletonema marinoi* CBA4 (B).

164x239mm (212 x 212 DPI)

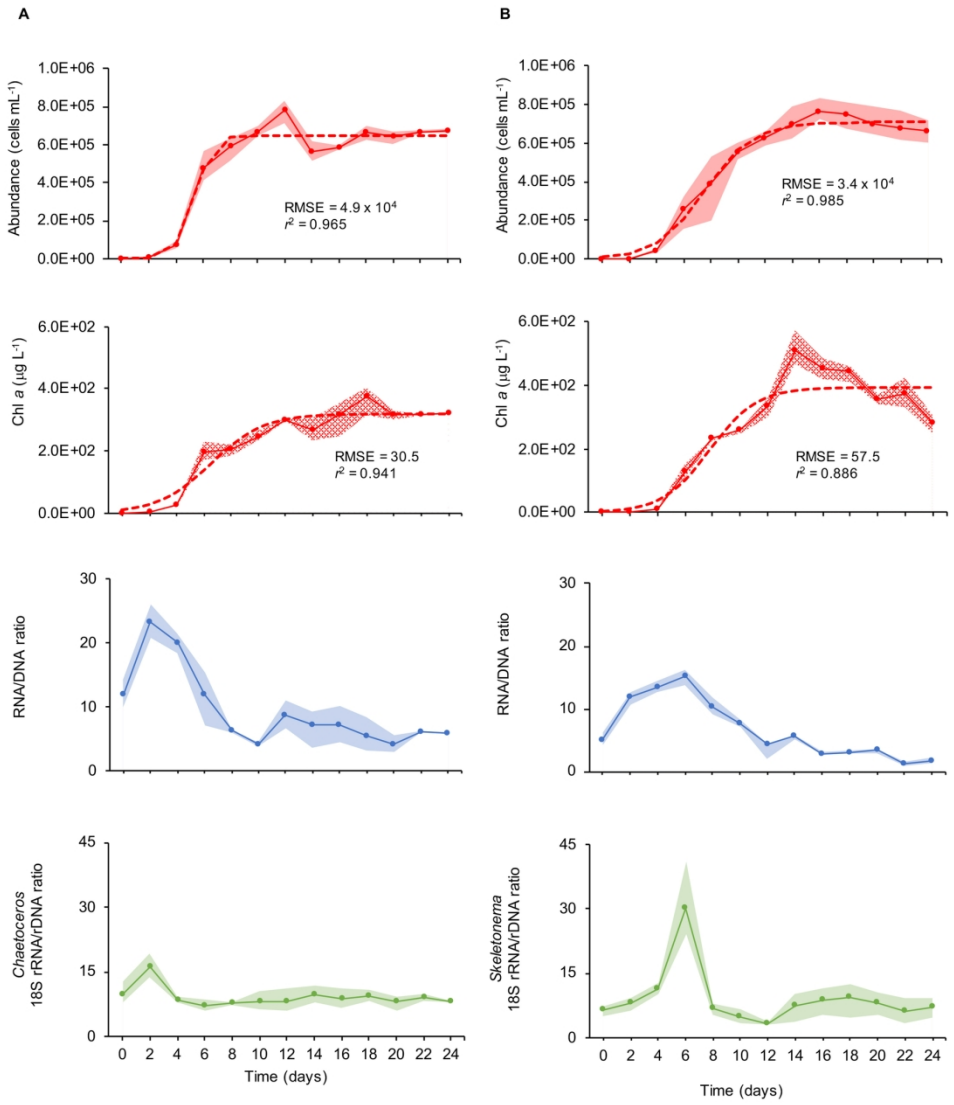

Figure 2. Growth curve of *Chaetoceros socialis* CBA22 (A) and *Skeletonema marinoi* CBA4 (B) expressed as biomass using abundance (cells mL^{-1}) and as chl *a* (µg L^{-1}), and RNA/DNA and taxon specific 18S rRNA/rDNA molecular ratios. Full and dotted red: biomass; blue: RNA/DNA ratio obtained by extracted nucleic acid concentrations; green: *Chaetoceros* and *Skeletonema* 18S rRNA/rDNA ratio. Red dotted line: logistic curve fitted to biomass data. Root mean square error (RMSE) and coefficient of determination (r^2) for abundance and chl *a* were shown, respectively. For each variable, colored areas are delimited by minimum and maximum values. All experiments were conducted in triplicate.

163x183mm (300 x 300 DPI)

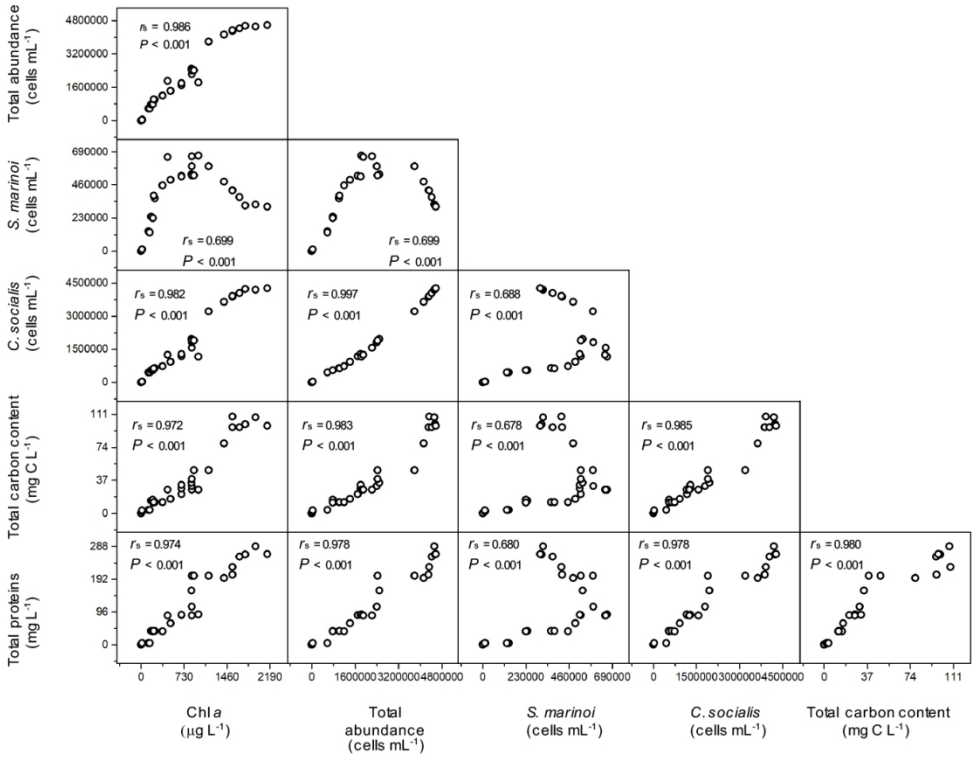

Figure 3. Matrix plot showing bivariate relationships among abundance, chl *a*, carbon content and total proteins as scatterplots for *Chaetoceros socialis* CBA22 and *Skeletonema marinoi* CBA4 in co-culture experiments.

164x128mm (217 x 217 DPI)

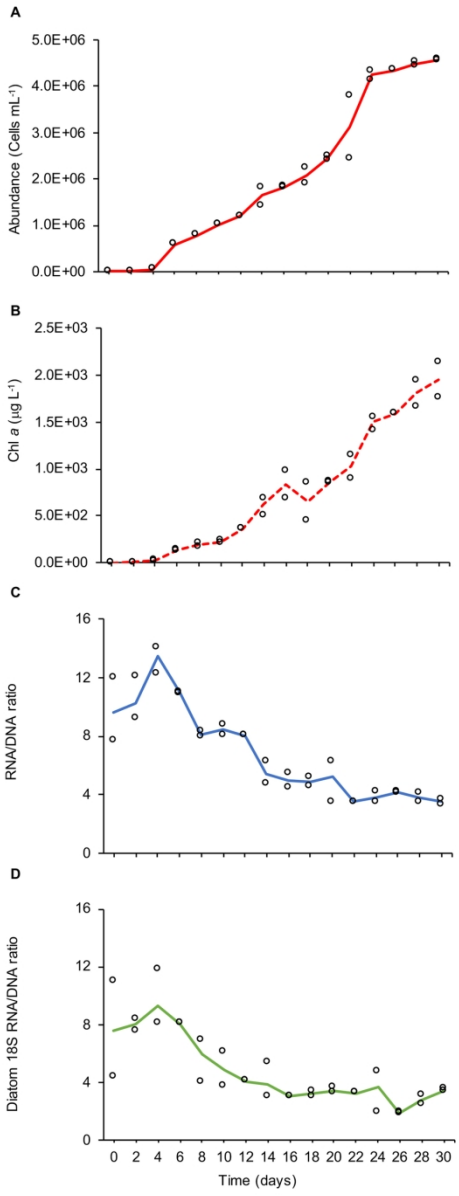

Figure 4. Growth curve of *Chaetoceros socialis* CBA22 and *Skeletonema marinoi* CBA4 in co-culture condition analyzed as total biomass using abundance (cells mL^{-1}) (A) and chl *a* (µg L^{-1}) (B), molecular total RNA/DNA (C) and diatom 18S rRNA/rDNA (D) ratios. Circles represented minimum and maximum values for each variable. All experiments were conducted in triplicate.

80x205mm (300 x 300 DPI)

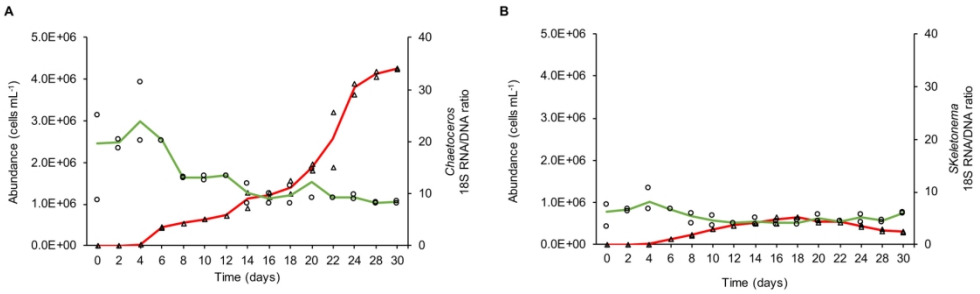

Figure 5. Growth curve in mixed cultured conditions analyzed based on abundance (cells mL^{-1}) and molecular ratios of *Chaetoceros socialis* CBA22 (A) and *Skeletonema marinoi* CBA4 (B). Red line represented mean values of abundance (cells mL^{-1}); green line represented mean values of *Chaetoceros* (A) and *Skeletonema* (B) 18S rRNA/rDNA ratio. Triangles and circles represent minimum and maximum values of cell abundance and 18S RNA/DNA ratios, respectively. All experiments were conducted in triplicate.

163x49mm (300 x 300 DPI)

Supplementary material

Table S1. List of genus-specific primer sequences of target diatom taxa targeting 18S rDNA regions, qPCR reagent concentrations, amplicon melting temperature (Tm) and size.

Taxon	Primer name	Forward primer sequence (5′–3′) Reverse primer sequence (5′–3′)	Primer concentration [nM]	$MgCl_2$ [mM]	Amplicon Tm (°C)	Amplicon size (bp)	Reference
Chaetoceros spp.	Chaet_spp_F	5′-ACTGAAGGGCAAGTCTGGTG-3′	300	1.5	84.52	132	This study
	Chaet_spp_R	5′-GAACCCACCAAAAGGTCGGA-3′					
Skeletonema spp.	Skel_spp_F	5′-ATTGGAGGGCAAGTCTGGTG-3′	300	1.5	83.76	118	This study
	Skel_spp_R	5′-TTGTGGTCAGTCACTCCTGC-3′					